Anisotropic Interpolation of Diffusion Tensor Images

A. Mishra[1], A. W. Anderson[1], J. C. Gore[1], Z. Ding[1]

[1]Institute of Imaging Science, Radiology & Radiological Science, Vanderbilt University, Nashville, TN, United States

Introduction

Fiber tracking with diffusion tensor imaging (DTI), in rigorous mathematical formulations, is the generation of continuous curves from a sampled direction field (1). The discrete nature of sampled data necessitates interpolation of the direction field for continuous curves to be obtained. This is particularly true for the DTI data, which are typically acquired at low spatial resolutions.

Interpolation is a classical image processing problem for which a variety of methods exist (2). The methods differ in frequency response, extent of support, computational complexity, and degree of continuity of the interpolated image. To date a few well established methods have been used for DTI data interpolation, which include low order polynomials (3, 4), cubic B-spline (1), and nearest neighbor interpolations (5). However, these methods suffer from either blurring or discontinuity artifacts most noticeably around structural boundaries in the interpolated image due to their imperfect frequency responses.

In this contribution, a novel method we have proposed for interpolating DTI data is described. Our primary considerations are preservation of structural boundaries and meanwhile assurance of continuity after interpolation. To satisfy the conflicting requirements, we developed an anisotropic interpolation technique that follows the provocative notion of anisotropic smoothing for enhancing flow-like structures (6). Presented herein are our preliminary studies on the behavior of this new interpolation technique, both in spatial and frequency domains, and comparisons with other DTI data interpolation methods based on in vivo human data.

Methods

DTI data typically contain a large number of fiber structures and hence boundary pixels. To smoothly interpolate the data with structural boundaries preserved, we developed an anisotropic mapping of the original image into an interpolated one. The equation below is the kernel function that governs the process of interpolation (see also Fig. 1 for kernel profiles and Fig. 2 for frequency responses). Essentially, the image intensities between neighboring pixels are interpolated based on the values of $\boldsymbol{a}$ and $\boldsymbol{\eta}$, with $\boldsymbol{a}$ controlling the sharpness of the kernel and η regulating the position of its maximum change in gradient. Suitably choosing these two parameters we can have a compromise between blurring and sharp discontinuity in edges using conventional interpolation schemes. In our design, we fix η to be 0.5, but $\boldsymbol{a}$ can be selected suitably to enclose desired high frequency components in the image that can preserve boundaries. For interpolation across fibers, where the intensity gradient is high, large values of $\boldsymbol{a}$ allow interpolation with a sharp transition. For interpolation along fibers, where the intensity gradient is low, small values of $\boldsymbol{a}$ allow smooth interpolation. By modulating the profile of the interpolation kernel with the local image intensity gradient as such, we can achieve an anisotropic interpolation that allows preservation of boundaries across fibers but smooth transitions along fibers.

$$f(g_i) = \frac{1}{1 + e^{a(\eta - g_i)}}$$

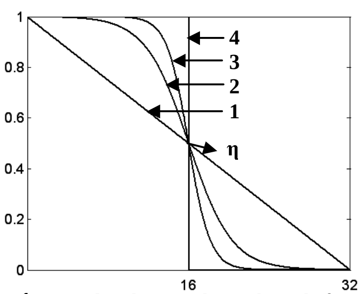

Fig. 1 Normalized interpolation kernels for 32 discrete values: 1. linear, 2. nonlinear with $\boldsymbol{a}$=10 and η =0.5, 3. nonlinear with $\boldsymbol{a}$ = 20 and η =0.5, 4. nearest neighbor.

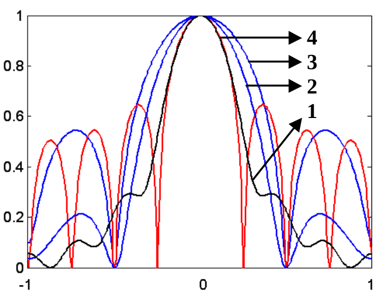

Fig. 2 Frequency response of interpolation kernels: corresponding to figure 1

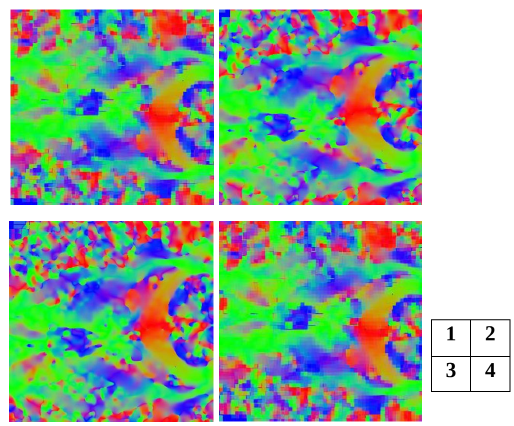

Fig. 3 Interpolated DTI data with the major eigenvector encoded in color using **1.** nearest neighbor, **2**. linear, **3.** cubic, and **4.** anisotropic interpolation.

Results

The anisotropic interpolation technique has been applied to in vivo DTI data acquired from a healthy human subject with a 3T GE Signa MR scanner (General Electric, Milwaukee, WI). The original in-plane resolution is 2x2 mm^2, but is anisotropically interpolated to be 0.25x0.25 mm^2. In this preliminary work, we used η = 0.5 and $\boldsymbol{a}$ = 16 to achieve anisotropic interpolation. The result is compared with those obtained by using nearest neighbor, linear and cubic interpolations (see Fig. 3). In Fig. 3, color encodes the direction of the major eigenvector of the interpolated DTI data, with sharp changes in color indicating boundaries of fiber bundles. In contrast to Fig.3.2 and 3.3, which has blurring around the boundaries, the new interpolation method preserves sharp structural boundaries, as shown in Fig. 3.4. Also compared to the nearest neighbor interpolation in Fig. 3.1, which has zero degree of continuity, the anisotropic interpolation we developed generates a tensor field that has a high degree of continuity.

Discussion and Conclusion

Preservation of structural boundaries is a prerequisite for accurate fiber tracking, i.e., confinement of fiber tracts within the anatomical structure. A continuous tensor field provides the basis for quantifying high order geometrical properties, such as curvature and torsion, of reconstructed fiber tracts. The anisotropic interpolation technique we developed can preserve structure boundaries and achieve a high degree of continuity. In addition, it has a compact support, reasonably low computational complexity, and superior frequency response compared to conventional interpolation methods. Our further studies are being conducted to optimize the parameter settings, evaluate the performance more comprehensively with synthetic and real data, and assess the impact of different interpolation methods on reconstructed fiber tracts.

Acknowledgements

This work was supported by NIH grants RO1EB02777 and RO1EB000461.

References

1. Basser PJ, et al. *Magn Reson Med* 2000:44:625-632.
2. Lehmann TM, et al. *IEEE Tran Med Imag* 1999:18:1049-1075.
3. Xu D, et al. *NeuroImage* 2002:17:1131-1143.
4. Gossl C, et al. *NeuroImage* 2002:16:378-388.
5. Mori S, et al. *Ann Neurol* 1999:45:265-269.
6. Weickert J. *Int J Comp Vision* 1999:31:111-127.